

Vortex flow in rotating superfluid $^3\text{He-B}$

L. Skrbek ^{a,b,1}, R. Blaauwgeers ^{a,c}, V.B. Eltsov ^{a,d}, A.P. Finne ^a, N.B. Kopnin ^{a,e},
M. Krusius ^a

^aLow Temperature Laboratory, Helsinki University of Technology, P.O. Box 2200, 02015 HUT, Finland

^bJoint Low Temperature Laboratory, Institute of Physics ASCR and Charles University, 18000 Prague, Czech Republic

^cKamerlingh Onnes Laboratory, Leiden University, P.O. Box 9504, 2300 RA Leiden, The Netherlands

^dKapitza Institute for Physical Problems, Kosygin 2, Moscow 117334, Russia

^eLandau Institute for Theoretical Physics, Kosygin 2, Moscow 117334, Russia

Abstract

For investigating vortex-line formation in rotating superfluid $^3\text{He-B}$ at high velocities of vortex-free superflow, the usual geometry is a cylindrical sample, which is connected via an orifice and a liquid ^3He column to the heat exchanger on the refrigerator. The orifice prevents vortex lines, created in the heat exchanger, from penetrating into the sample until the rotation velocity reaches a critical value Ω_c . We describe NMR measurements of Ω_c as a function of temperature and discuss the results in terms of vortex-line pinning at the rim of the orifice.

Key words: superfluid ^3He ; vortex dynamics; vortex formation; critical velocity; counterflow; Magnus force; mutual friction

Ideally in a superfluid rotating at constant angular velocity Ω , the existing vortices are contained in a central cluster of rectilinear lines, coaxial within a closed cylindrical container. Vortex containment is provided by the Magnus force from the macroscopic normal - superfluid counterflow which circulates between the cluster and the container wall. This is the hydrodynamically stable state of the superfluid in uniform rotation. The only residual motion is a slow diffusion of vortex lines towards a better annealed vortex lattice.

In practice the geometry of the sample container is more complicated (Fig. 1) and nonuniform vortex densities cannot be entirely avoided. Uncontrolled vortex motion may then become possible, in some cases even at constant Ω . This is the case at low temperatures in the B phase, when vortex-free counterflow states at high Ω are investigated. Here the uncontrolled flow of vortex lines through a small filling tube or aperture may prevent studies of vortex-line formation altogether.

We report on observations of the rotation threshold, the onset Ω_c , when vortices start to flow for the first time through the central orifice into the sample volume (Fig. 1). In the B phase, the orifice flow becomes the dominant mechanism of vortex formation which bypasses all other processes in a smooth-walled quartz container [1,2]. Fig. 2 displays our measurements of Ω_c as a function of temperature which in a narrow temperature interval exhibits a crossover between two different types of behavior.

In the high-temperature regime at $T > 0.55 T_c$ the first event of vortex flow into the vortex-free B phase is measured at (2.2 ± 0.3) rad/s, independently of temperature. The data are independent of prehistory, *ie.*, whether vortices have previously been in the sample or not, and they do not correlate with the sequence of rotation directions which have been in use before. This means that remnant vortices, which would be trapped somewhere on the walls, are probably not present on the smooth annealed quartz walls of our container. In contrast to low temperatures, in the high-temperature regime Ω_c is largely insensitive to rotational acceleration, $\dot{\Omega} \sim (0.25 \dots 4) 10^{-3}$ rad/s², which is used for

¹ E-mail: skrbek@fzu.cz

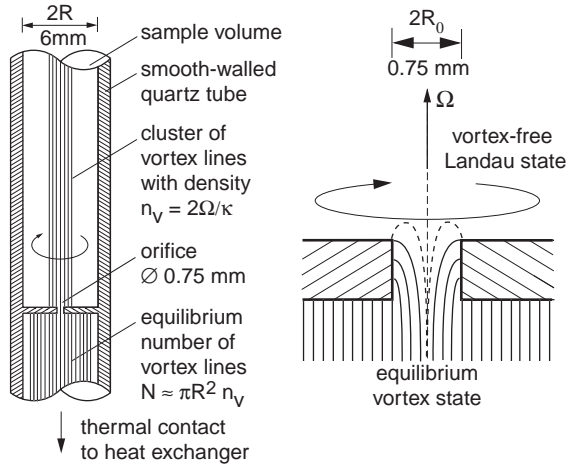


Fig. 1. (Left) Long cylindrical container [2], shown here with a vortex cluster in the sample volume. (Right) In measurements of vortex formation, the sample volume is kept in vortex-free counterflow while vortex lines crowd the orifice which connects the sample to the refrigerator.

sweeping up Ω , when one scans for the threshold. In the low temperature regime below $0.55 T_c$, Ω_c decreases sharply to a low level (Fig. 2), which depends on the acceleration $\dot{\Omega}$ and the noise spectrum of the rotation drive $\Omega(t)$.

The leak through the orifice results in a cluster with a relatively large and variable number of rectilinear vortex lines. At $0.75 T_c$ typically 50 or more vortex lines are formed. This exceeds the number of vortex lines which at Ω_c fit inside the orifice in solid-body rotation. Towards low temperatures the number of vortex lines in the first leak increases and below $0.5 T_c$ the leak essentially removes all excess vortex-free counterflow. Thus at low temperatures, where mutual friction damping of vortex motion becomes small, the leak leads to a rapid multiplication of vortices [3]: Vortex lines in the orifice first extend as loops into the sample volume, these then intersect each other, and finally evolve into a vortex tangle by reconnecting. For a short moment this process mimics superfluid turbulence, multiplying the yield of vortex lines. The rapid increase in the yield of vortex lines with decreasing temperature is typical of all dynamic processes which lead to vortex-line formation from initial small loops in large vortex-free counterflow [3]. This is particularly true of the low-temperature orifice leak in Fig. 2. The combination of high yield and low onset makes many types of measurements on vortices as a function of Ω impossible below $0.5 T_c$.

One might think that a small vortex cluster above the orifice would efficiently block any further flow from the orifice. However, our measurements show that the cluster does not essentially increase the onset of the leak in the temperature regime of Fig. 2. During a slow

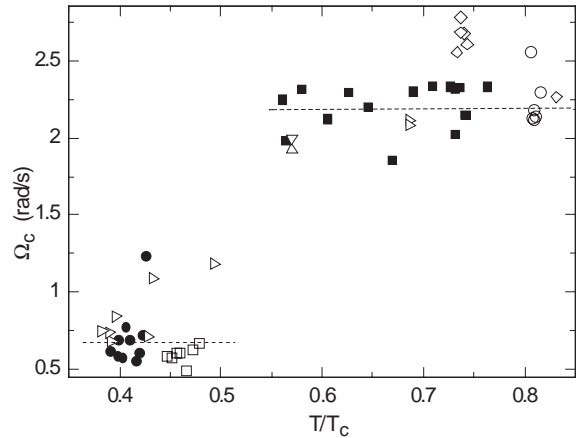


Fig. 2. Measurements on the first event of vortex flow through the orifice, with vortex-free superflow in the sample volume: the onset velocity Ω_c plotted as a function of temperature below the A→B transition at 29 and 34 bar pressure. The data have been measured by sweeping Ω upward at a rate $\dot{\Omega} \leq 4 \cdot 10^{-3} \text{ rad/s}$. Different symbols represent data from different measuring runs. The lines illustrate average behavior, emphasizing the crossover between two different regimes.

upward sweep of Ω , separated events of orifice flow thus occur successively as a function of Ω above the onset Ω_c . Above $0.55 T_c$ their spacing is roughly of order Ω_c while at low temperatures the spacing is smaller and less consistent. The fact that the vortex cluster does not more efficiently block the orifice probably reflects the inhomogeneous local velocities around the orifice while Ω is scanned upwards.

The onset of vortex motion in the orifice of Fig. 1 can be estimated with scaling arguments which lead to a Feynman formula for vortex depinning. During increasing rotation we may assume that vortex lines fill the space below the orifice at equilibrium density. The first vortex starts to creep up inside the orifice when Ω exceeds some critical value Ω_0 , which can be estimated as follows: The line tension (or kinetic energy of vortex circulation per unit length) of the vortex is $\epsilon_v = (\rho_s \kappa^2 / 4\pi) \ln(r_v/r_c)$, where $\kappa = h/(2m_3) = 0.066 \text{ mm}^2/\text{s}$ is the circulation quantum, $r_v \approx 1/\sqrt{n_v}$ denotes the inter-vortex distance and $n_v = 2\Omega/\kappa$ is the vortex-line density within a vortex cluster in solid-body rotation, while $r_c \approx \xi(T, p) \sim 10 \text{ nm}$ is the vortex core parameter. At the lower rim of the orifice the vortices are bent. Their curvature is determined by the balance between line tension and the Magnus force which is created by the vortex-free counterflow in the orifice: $\epsilon_v k = \kappa \rho_s v_s$, where k is the local curvature of the vortex lines. We find that a vortex line which terminates at the lower rim is stable until

$$\Omega_0 \approx \frac{\kappa}{4\pi R_0^2} \ln \frac{r_v}{r_c} \quad (1)$$

where R_0 is the radius of the orifice. For our geometry

$\Omega_0 \approx 0.4$ rad/s. At higher rotation velocities the vortex is pulled inside the orifice and then creeps to the upper rim. Here it remains pinned with one end at the upper rim until its radius of curvature decreases close to $R_0/2$, the situation depicted with dashed lines in the right half of Fig 1. A crude estimate of the rotation velocity needed to pull vortices away from the upper rim of the orifice can be obtained if one substitutes R_0 with $R_0/2$ in the expression for Ω_0 . This leads to the estimate $\Omega_c \approx 1.4$ rad/s, independently of temperature and in reasonable agreement with the measurements in Fig. 2 in the high temperature regime.

Except for a weak logarithmic factor, Ω_c scales with the size of the orifice as $1/R_0^2$. The choice of the radius R_0 is a compromise between sufficient thermal contact and a high enough Ω_c . An earlier attempt with a larger orifice produced less consistent data, but experimentally no vortex-free rotation was observed above 1.4 rad/s. The calculated estimate for $R_0 = 0.5$ mm gives $\Omega_c \approx 0.8$ rad/s. Overall, the high-temperature data in Fig. 2 thus seem to support the scaling argument for Ω_c .

In the crossover regime ($0.50 \dots 0.55$) T_c mutual-friction damping of vortex motion is exponentially dropping with decreasing temperature. This fact accounts for the sudden drop in the stability of orifice pinning below $0.55 T_c$ and its sensitivity to fluctuations in the rotation drive.

The flow of vortex lines through tubes and apertures is a difficulty which in $^3\text{He-B}$ often dominates vortex formation. It is surprising to find that its measurements yield as consistent results as those in Fig. 2.

This collaboration was carried out under the EU-IHP programme (ULTI 3) the ESF network COSLAB.

References

- [1] R. Blaauwgeers *et al*, preprint arXiv:cond-mat/0111343 and these proceedings.
- [2] R. Blaauwgeers *et al*, these proceedings.
- [3] A.P. Finne *et al*, these proceedings.